# Quantitative and specific recovery of natural organic and mineral sulfur for (multi-)isotope analysis

I. Jovovic, V. Grossi, Pierre Adam, L. Simon, I. Antheaume, F. Gelin, M. Ader, P. Cartigny

# Quantitative and Specific Recovery of Natural Organic and Mineral Sulfur for (Multi-)Isotope Analysis

I. Jovovic[1]*, V. Grossi[1], P. Adam[2], L. Simon[3], I. Antheaume[1], F. Gelin[4], M. Ader[5], P. Cartigny[5]

[1]Laboratoire de Géologie de Lyon, Univ Lyon, Univ Lyon 1, ENSL, CNRS, LGL-TPE, F-69622, Villeurbanne, France

[2]Université de Strasbourg, CNRS, Institut de Chimie de Strasbourg UMR 7177, F-67000 Strasbourg, France[3]Univ Lyon, Université Claude Bernard Lyon 1, CNRS, ENTPE, UMR 5023 LEHNA, F-69622, Villeurbanne, France[4]Unconventional R&D Program, TOTAL E&P, Centre Scientifique et Technique Jean Féger, 64018 Pau, France

[5]Université de Paris, Institut de physique du globe de Paris, CNRS, F-75005 Paris, France

*corresponding author: ivan.jovovic@univ-lyon1.fr

**ABSTRACT**

Deciphering the role of sulfur in biogeochemical cycles strongly relies on its stable isotope composition, which ultimately depends on the ability to quantitatively recover different sulfur species from geological samples. For decades most studies have been restricted to the $^{34}S/^{32}S$ composition of bulk samples, using simple methods based on the analysis of $SO_2$ released by sample combustion combined to mass spectrometry. The wet chemistry procedures required to selectively extract specific sulfur species were generally avoided due to their tediousness and inefficiency for some complex matrices, especially when targeting organic sulfur. With the recent advent of multi-isotope studies (investigating the minor sulfur stable isotopes $^{33}S$ and $^{36}S$) which rely either on the analysis of sulfur as $SF_6$, or on the use of secondary ion or multi-collector inductively coupled plasma mass spectrometry, wet chemistry-based

preparation procedures were brought back to the stage with a renewed interest in developing procedures better adapted to the investigation of specific sulfur species.

Here we propose a new stepwise chemical procedure for the quantitative recovery and multi-isotope analysis of organic sulfur from both solvent soluble (total lipid extract) and insoluble (kerogen) fractions, based on a wet oxidation by sodium hypochlorite. This procedure also allows the multi-isotope analysis of inorganic sulfur species (elemental sulfur, sulfates and sulfides) in the same sample. Its application to different well-known petroleum source rocks and to an oil demonstrates its relevance for disentangling the interactions between the different sulfur pools and for shedding new light on the sulfur biogeochemical cycle.

**Keywords : sulfur (multi-)isotopes; organic and mineral sulfur; source rocks; chemical oxidation of organic sulfur; S biogeochemical cycle**

## 1. INTRODUCTION

Sulfur (S) is a key element of biogeochemical cycles, being both an essential component of living cells and involved in major geological processes. The proportions of its four stable isotopes ($^{32}S$, $^{34}S$, $^{33}S$, $^{36}S$, in order of natural abundance) vary upon equilibrium and/or kinetic conditions, and can be used as tracers of S biogeochemical cycles and processes (Passier et al., 1999; Canfield, 2001; Johnston, 2011). S-isotope compositions are expressed as per mil (‰) differences relative to the isotopic composition of the Vienna Canyon Diablo Troilite international standard (V-CDT), and presented in standard δ notation: $\delta^{A}S = {}^{A}R_{sample}/{}^{A}R_{CDT} - 1$ where $^{A}R = {}^{A}S/{}^{32}S$ and A = 33, 34 or 36 (note however that there is not yet any international standard for the $^{33}S/^{32}S$ and $^{36}S/^{32}S$ ratios).

The three isotope ratios ($\delta^{33}S$, $\delta^{34}S$ and $\delta^{36}S$) primarily scale on their relative mass differences and their fractionation can be predicted using an approximation of their partition function

(Bigeleisen and Mayer, 1947; Young et al., 2002). This is known as mass-dependent fractionation: $\delta^{33}S \approx 0.515 \times \delta^{34}S$ and $\delta^{36}S \approx 1.89 \times \delta^{34}S$ (see thereafter for more formal and rigorous equations). However, most studies solely focus on $^{34}S$ fractionation, which is the easiest to measure. Such measurements have become common with the development of elemental analysis coupled to isotope ratio mass spectrometry (EA-IRMS), in which S is oxidized to $SO_2$, and the $^{34}SO_2/^{32}SO_2$ ratio subsequently measured (Giesemann et al., 1994). EA-IRMS analyses of $\delta^{34}S$ are low cost, easy and fast to operate. Though, the oxygen interferences inherent to the use of $SO_2$ gas forbid reliable multi-isotope approaches (Rees, 1978).

More recently, multi-isotope studies have enlightened previously poorly constrained atmospheric and (bio)(geo)chemical processes (Farquhar et al., 2000; Farquhar and Wing, 2003; Luo et al., 2018). For instance, the specific $^{32}S$, $^{33}S$, $^{34}S$ and $^{36}S$ signatures of ancient rocks led to a new understanding of Archean and Paleoproterozoic atmospheric chemistry and S cycling (Farquhar et al., 2000; Philippot et al., 2007). The analysis of $^{33}S$ and $^{36}S$ isotope compositions was also a key factor in achieving a better understanding of hydrothermal processes (Ono et al., 2007) and microbial metabolic pathways such as sulfate reduction, S oxidation and S disproportionation (*e.g.* Farquhar et al., 2003; Johnston et al., 2005; Ono et al., 2006). The interpretations rely on both the (small) deviations in the behavior of each S-isotope and mass-conservation effects which are expressed using the conventional $\Delta$ notation: $\Delta^{33}S = \delta^{33}S - [(\delta^{34}S + 1)^{0.515} - 1]$ and $\Delta^{36}S = \delta^{36}S - [(\delta^{34}S + 1)^{1.89} - 1]$. As for any isotope method, the determination of the multi-isotope composition of specific S species in a given sample (*e.g.* sulfates, sulfides, elemental sulfur ($S^0$), organic sulfur; Table 1) requires the quantitative recovery and purification of the different S pools. Sulfides (and/or acid volatile S), sulfates and $S^0$ are typically recovered as $Ag_2S$ using distillation methods and reducing solutions (Thode et al., 1958; Pepkowitz and Shirley, 1950; Forrest and Newman, 1977;

Canfield et al., 1986). Each targeted S-pool is first converted into $H_2S$ by an adapted acid treatment, and subsequently recovered as a solid metal sulfide (typically as $Ag_2S$, sometimes as ZnS or CdS). The obtained metal sulfide is then transformed into either $SO_2$ or $SF_6$ (*e.g.* Thode et al., 1961; Thode and Rees, 1971, respectively) and analyzed by IRMS. Contrary to oxygen, fluorine has only one stable isotope. Because it avoids the need for $^{17}O$ or $^{18}O$ corrections (Rees, 1978), IRMS analysis of $SF_6$ is more precise and accurate and, accordingly, has been preferentially used to investigate all four S stable isotopes (Hulston and Thode, 1965). This, however, requires a non-automated conversion of $Ag_2S$ into gaseous $SF_6$ and the purification of the latter. Alternatively, the use of secondary ion mass spectrometry (SIMS) has been proposed for the *in-situ* analysis of $^{32}S$, $^{33}S$ and $^{34}S$ (*e.g.* Thomassot et al., 2009; Whitehouse, 2012), and multi-collector inductively coupled mass spectrometry (MC-ICPMS) has been used for the determination of $^{32}S$, $^{33}S$ and $^{34}S$ contents in small purified samples (*e.g.* Albalat et al., 2016). SIMS is however less available and requires specific standards. Though high precision measurements of $^{34}S$ can be obtained with MC-ICPMS (*e.g.* Paris et al., 2013), this technique is hardly as precise as IRMS analysis of $SF_6$ for $^{33}S$-measurements and cannot provide $^{36}S$ data.

Organic sulfur ($S_{org}$) is, after pyrite, the second most abundant reduced S pool in sediments (Anderson and Pratt, 1995), where it usually occurs as a complex mixture of monomeric and polymeric organosulfur compounds (OSC). Sedimentary $S_{org}$ can be further divided into a soluble (solvent-extractable) and an insoluble (non-extractable or residual) OSC-pools. Biosynthetic $S_{org}$ mainly occurs as chemically labile proteins and amino acids that are expected to be quickly degraded during diagenesis (Tissot and Welte, 1984 ; Kutuzov et al., 2019) though, in some cases, they could contribute their sulfur atoms to the kerogens (Raven et al., 2018). On the other hand, $S_{org}$ in recent sediments typically increases with depth. For example, Werne et al. (2003) showed an increase from 0.05 to 0.12 of the organic S/C ratio in

the Cariaco Basin with sediment depth. This increase reflects a diagenetic S-enrichment of organic matter by sulfurization processes (natural vulcanization) which involve reduced S species produced by microbial sulfate reduction (MSR; Sinninghe Damsté et al., 1989; Adam et al., 1993). The idea of a common source of sedimentary $S_{org}$ and mineral S (usually pyrite) is further supported by their respective $\delta^{34}S$ signatures generally depleted relative to sulfates (*e.g.* Thode et al., 1958; Zaback and Pratt, 1992; Tuttle and Goldhaber, 1993; Canfield et al., 1998; Werne et al., 2003). However, $S_{org}$ is still often $^{34}S$-enriched relative to pyrite (*e.g.* 10-20‰ in marine sediments, Orr, 1986; 5-8‰ in Cariaco Basin, Werne et al., 2003). Tuttle (1991), then Werne et al. (2003) explained this relative enrichment by a delayed sulfurization of organic matter relative to the formation of pyrite, but this simple view likely overlooks the fact that different organic molecules may react with reduced species at different rates depending on the context (*e.g.* Amrani, 2014, Raven et al., 2016a, Raven et al., 2016b, Shawar et al., 2020).

Thus, our understanding of the biogeochemical S cycle still remains incomplete and could clearly benefit from $S_{org}$ multi-isotope analyses, but only few dedicated studies have been performed so far (*e.g.* Oduro et al., 2011, Labidi et al., 2017, Siedenberg et al., 2018). Reasons are linked to the structural diversity and distinct solubilities of biological and geological OSC, and to their difficult clear-cut separation from the inorganic S pools, which make them more arduous to recover specifically and quantitatively. In this respect, an adapted procedure for the specific and quantitative recovery of $S_{org}$ would also be useful for studies dedicated to $^{34}S_{org}$ signatures. Most existing procedures for the release of $S_{org}$ rely on its oxidation into sulfates by combustion methods such as Eschka fusion (using a 2:1 mixture of MgO and $Na_2CO_3$ at *ca.* 900°C, Eschka, 1874), or $Na_2O_2$ Parr bomb and $Br_2$ oxidations, with yields close to 100% and a good replicability (Selvig and Fieldner, 1927; Siedenberg et al.,

2018). However, those methods are tedious, dangerous and difficult to apply routinely to large sets of samples.

More recently, some studies have introduced the use of specific methods to improve $S_{org}$ recovery for (multiple) S-isotope measurements (Table 1). For instance, Oduro et al. (2011) used Raney nickel as a catalyst for the desulfurization of volatile OSC and the recovery of $S_{org}$ as nickel sulfide. Though they showed yields close to 100% for the desulfurization of many volatile OSC, this method did not appear suitable for the recovery of sulfones. Moreover, Raney nickel is a solid which poorly reacts with insoluble OSC from kerogens. To our knowledge, none of the presently available procedures allows a simple, selective and quantitative recovery of both mineral S and $S_{org}$ pools.

Here we propose a new stepwise chemical procedure for the selective and quantitative recovery as $Ag_2S$ of solvent-extractable and non-extractable $S_{org}$ from sediments and oils, applicable for a specific and reliable determination of either $^{34}S$ or the multiple S-isotope composition of distinct $S_{org}$ pools. It relies on oxidation of organic matter with sodium hypochlorite (NaOCl), which was previously shown to release organic-bound S as sulfates (*e.g.* Li and Cho, 2005). This procedure is further compatible with the analysis of sulfides, sulfates and $S^0$ in the same samples. The complete optimized procedure was carefully tested on an oil and sediment samples from lacustrine and marine environments of various ages (from modern to 50 Myr), validating its suitability for the (multi-)isotope analysis of geological organic and mineral S and allowing a new model of the S cycle to be considered for some depositional environments.

## 2. MATERIAL AND METHODS

### 2.1. Samples

Due to the large diversity of S forms in nature, their distinct reactivity and potential interaction with natural matrices, our method was developed and tested on several natural samples rather than pure minerals and OSC. These samples were selected among organic matter- and S-rich sediment formations from various locations, and complemented with a S-rich oil (Table 2).

We selected sediments from the Eocene Green River Fm Mahogany Zone (Utah, USA, Bradley, 1964; Smith and Carroll, 2015; Tuttle, 1991), and sub-superficial sediments from the modern Lake Dziani Dzaha (Mayotte, Indian Ocean, Leboulanger et al., 2017; Milesi et al., 2020). A marine shale sample from the Miocene Monterey Fm (California, USA, Orr, 1986; Zaback and Pratt, 1992) was added to the sample set. Lastly, we used a sample from Rozel Point seeps (Utah, USA, Thode et al., 1958; Eardley, 1963; Mauger et al., 1973) to evaluate the efficiency of the new method on pure organic matter. A non-referenced sample from the Limagne Basin (Massif Central, France, Wattinne et al., 2003; Seard et al., 2013) was added to compare the yields of $S_{org}$ obtained with Raney nickel (Oduro et al., 2011) and the newly developed method (Table 3).

None of these samples was thermally mature except for the Rozel Point oil seep sample for which maturity was hardly defined (Eardley, 1963); thermal maturation effects on $S_{org}$ recovery is therefore not discussed in this study.

## 2.2. Analytical steps

Samples were freeze dried, ground to <100 µm, and homogenized. Subsamples (*ca.* 1 g) were then subjected to a sequence of chemical extractions in order to specifically recover the different organic (soluble and insoluble) and mineral ($S^0$, sulfates, sulfides) S pools (Fig. 1).

Only Pyrex glassware was used and all chemicals were reagent-grade. Dilutions and washes were performed in 100 mL centrifuge tubes using deionized water. S-purity of all reagents

was regularly checked and considered as acceptable when less than 5 µg of S was recovered in a whole blank procedure.

### *2.2.1. Solvent extraction and $S^0$ precipitation*

The soluble organic matter was extracted by multiple sonication cycles (10 minutes each) with methanol (MeOH, twice), dichloromethane (DCM):MeOH (1:1, v/v, twice) and DCM (twice) at room temperature (*ca.* 20°C). The total lipid extract (TLE) was treated with activated copper curls to precipitate $S^0$ as $Cu_xS_y$ (Blumer, 1957).

### *2.2.2. Reducing distillations*

The acidic $CrCl_2$ (Canfield et al., 1986) and STRIP (Forrest and Newman, 1977; Pepkowitz and Shirley, 1950; Thode et al., 1961) solutions have been extensively used for the extraction of mineral S compounds in samples from a wide range of natural settings and laboratory experiments. Gröger et al. (2009) have shown that the $CrCl_2$ solution typically converts 99±1 % of both sulfides and $S^0$ into $H_2S$, but hardly reacts with individual OSC and sulfates (typical yields <0.2 %). However, since the reactivity of the $CrCl_2$ solution has never been tested against very fresh natural OM, the eventuality of a reaction with some OSC, *e.g.* organic polysulfides cannot be totally excluded. Moreover, Arnold et al. (2014) have shown that the STRIP solution typically yields close to 100 % of both sulfides and sulfates, but hardly converts OSC to $H_2S$. Therefore, the $CrCl_2$ solution was used to selectively recover sulfide-S and $Cu_xS_y$-S, whereas the STRIP solution was used to recover sulfate-S from sulfide-free samples.

Due to its sensitivity towards oxidation, the $CrCl_2$ solution was prepared daily according to Fossing and Jorgensen (1989). A glass bottle closed with a teflon-coated rubber cap was filled with a an acidic $CrCl_3$ solution (80 ml of 3 % HCl and 21.15 g $CrCl_3$, 6 $H_2O$). The Cr(III)

198 solution was then reduced to Cr(II) by the addition of zinc granules (14 g). The solution was
199 stirred under a nitrogen flush until the initial dark green color had completely turned to bright
200 blue.
201 The STRIP solution is more stable and was used within 6 months after preparation. A glass
202 Erlenmeyer flask was filled with 523 ml of 37 % HCl, 321 ml of 57 % hydriodic acid (HI)
203 and 156 ml of 50 % hypophosphorous acid ($H_3PO_2$). The solution was heated under a nitrogen
204 flush and gently refluxed, for 6 hours.
205 The apparatus that was used for S distillation is represented in Fig. 2. We ensured that the
206 treated sample did not contain more than *ca.* 125 µmol S to guarantee a large excess of
207 reagents and allow the reaction to be quantitative. The targeted S pool was converted to $H_2S$
208 with either 10 mL of 37 % HCl and 25 mL of $CrCl_2$ solution (sulfides/$S^0$) or 25 mL of STRIP
209 solution (sulfates), and refluxed for 3 hours. Produced $H_2S$ was purged and precipitated as
210 $Ag_2S$ in a silver nitrate trap (20 ml of 2.48 % $AgNO_3$). A few drops of a 25 % ammonia
211 solution were added to the the $Ag_2S$ precipate, which was then centrifuged, washed three
212 times with 30 ml of deionized water, and lyophilized. The dry $Ag_2S$ powder was stored out of
213 sunlight before fluorination and S multi-isotope analysis.
214
215 *2.2.3. Oxidation of organic matter*
216 The mineral S-free sediments/oils and $S^0$-free TLE were heated at 60 °C under stirring with a
217 10-15 % NaOCl solution in a 100 mL centrifuge Pyrex tube. It is noteworthy that, even under
218 reflux and stirring, concentrated NaOCl easily tends to evaporate, resulting in a poor
219 reactivity, especially over long reaction times. Therefore, the solution was kept under 70 °C.
220 To guarantee a large excess of hypochlorite ions, we introduced no more than *ca.* 125 µmol S
221 and *ca.* 25 mmol C from each sample for 25 ml of NaOCl solution. Various treatment times
222 (6, 12, 24 and 48 hours) were tested to evaluate the reaction kinetics. This oxidative digestion

of organic matter resulted in the liberation of $S_{org}$ from solvent-soluble or insoluble organic matter as sulfates. After reaction, the solution was carefully acidified with 37 % HCl, until pH <2, to allow the consumption of excess hypochlorite ions and carbonate by-products, and to facilitate the precipitation of sulfates. Sulfates were precipitated as $BaSO_4$ using 20 mL of a saturated $BaCl_2$ solution (>360 $g.L^{-1}$). The resulting precipitate was centrifuged and rinsed twice with 20 mL of the saturated $BaCl_2$ solution, than freeze dried and homogenized before distillation as illustrated in 2.2.2.

*2.2.4. TOC and GC-MS analyses*

The evolution of total organic carbon (TOC) contents in residual sediments during digestion was monitored using an elemental analyzer (Vario ISOTOPE Select, Elementar) equipped with a Thermal Conductivity Detector. The accuracy of the measurements was evaluated using an international sediment standard, namely IVA33802151 (TOC = 9.15 %).

Residual aqueous phases after oxidation with NaOCl were extracted with DCM and ethyl acetate, successively, to investigate the potential soluble organic compounds freed by the process. The extracts were then derivatized with diazomethane and analyzed by gas chromatography coupled to mass spectrometry (GC-MS), using a Thermo Trace gas chromatograph coupled to a Thermo TSQ Quantum mass spectrometer operating in the electron ionization mode (70 eV) and scanning *m/z* 50 to 700. The temperature of the source was set to 220 °C. Gas chromatographic separations were performed on a HP5-MS column (30 m length with 0.25 mm diameter and 0.1μm film thickness) with helium as carrier gas (1.1 $mL.min^{-1}$). The temperature program was: 40°C (10 min), 40-300 °C (6 $°C.min^{-1}$), isothermal at 300 °C (25 min).

*2.2.5. Isotope analyses*

The $Ag_2S$ powders corresponding to the different organic and mineral S pools were freeze dried, homogenized and weighed in aluminum boats before being fluorinated overnight in Nickel bombs with excess fluorine gas at 350°C. The produced $SF_6$ was purified cryogenically and by subsequent gas chromatography prior to the determination of its $\delta^{33}S$, $\delta^{34}S$ and $\delta^{36}S$ values using a Thermo Scientific MAT 253 dual-inlet IRMS (Au Yang et al., 2016). The accuracy of the measurements was evaluated using an international $Ag_2S$ standard, namely IAEA-S1 (also known as Vienna-CDT), with a $\delta^{34}S$ value = -0.3 ‰. Typical analytical deviations were below 0.01 ‰ and 0.1 ‰ for $\delta^{33}S$ or $\delta^{34}S$ and $\delta^{36}S$ values, respectively, and ≈ 0.005 ‰ and 0.1 ‰ for $\Delta^{33}S$ and $\Delta^{36}S$ values, respectively (1σ).

Total sulfur contents (TS) and associated $\delta^{34}S$ values were measured with a VarioPYROcube elemental analyzer (Elementar) in NCS combustion mode interfaced in continuous-flow mode with an Isoprime 100 IRMS (Fourel et al., 2014). The accuracy of those measurements was evaluated using the aforementioned international $Ag_2S$ standard and one international $BaSO_4$ standard (NBS-127, $\delta^{34}S$ value = +20.3 ‰). Typical analytical deviations were below 0.05 % and 0.3 ‰ for the TS and $\delta^{34}S$ values, respectively (1σ).

## 3. RESULTS AND DISCUSSION

### 3.1. Procedure validation

Subsamples were first used to test and optimize the oxidation procedure of $S_{org}$ with NaOCl. Then, triplicates of most samples were treated with the full stepwise procedure (Fig. 1 and Table 2). Using a mass balance calculation, the results of the triplicate analyses were compared to those obtained by direct EA-IRMS analysis of the dry sediments as a quantitative validation of the overall analytical workflow.

#### *3.1.1. $S_{org}$ oxidation to sulfates and recovery*

Figure 3 shows the evolution of the carbon- and sulfate-contents in TLE and mineral-S free kerogens during 48 hours of NaOCl oxidation at 60°C. Within 24 hours, less than 7 ±3 % of the initial carbon remained in the sample, and more than 95 ±5 % of $S_{org}$ was recovered as sulfates. The GC-MS analysis of residual organic compounds in aqueous phases after 4 and 12 hours of oxidation showed the occurrence of carboxylic diacids (> 4 carbons), chlorinated carboxylic monoacids as well as chlorinated and non-chlorinated benzene carboxylic polyacids (up to hexa-acids). Those products are expectable during the oxidation of organic matter with NaOCl (Wang et al., 2014). More importantly, no OSC (*e.g.* thiols, thiophenes, sulfoxides, sulfones, sulfonic acids, thioesters, polysulfides) was identified in any aqueous phase, showing an efficient oxidation of S bound to organic matter into recoverable sulfates. It cannot be excluded, however, that some OSC in other matrixes may react less efficiently, thus requiring a longer reaction time to be entirely oxidized.

The remaining $S_{org}$ recovered after 6, 12, 24 and 48 hours revealed no significant isotope evolution associated with the oxidation process (Fig. 4). This suggests that the progressive organic matter digestion is not associated with significant isotope effects, and that an incomplete oxidation of $S_{org}$ in samples would not impact S isotopes measurement –though quantitative aspects should not be considered in this case.

For some samples, the yield of $S_{org}$ obtained with our new method was compared with that obtained with the Raney nickel desulfurization method used by Oduro et al. (2011). Much higher yields were obtained with the new method for soluble $S_{org}$ (7 to 200 times, Table 3), which can be explained by a possible high steric hindrance of $S_{org}$ in these specific samples. Unsurprisingly, due to the low kinetics of unfavorable solid-solid reactions, the new method was also significantly more efficient for the insoluble $S_{org}$ present in kerogens, compared with the 4-times lower recovery of this S pool using Raney nickel (Table 3). None of the quantities

297 of $S_{org}$ recovered with Raney nickel were sufficient for the determination of S isotopic
298 composition with Fluorination-IRMS.
299
300 *3.1.2. Mass balance validation*
301 The TS content and bulk $\delta^{34}S$ value measured for each bulk sample were compared to those
302 calculated from the S multi-pool analysis of the same sample (triplicate analyses), using the
303 following mass balance equation : $\%S_{total} \times \delta^{34}S_{total} = \Sigma(\%S_i \times \delta^{34}S_i)$, where *i* is in {soluble
304 $S_{org}$, insoluble $S_{org}$, $S^0$, sulfides, sulfates}.
305 The results are presented in Figure 5. The very good consistency between the two approaches
306 ($RMSE_{TS}$ = 0.13 % and $RMSE_{\delta 34S}$ = 1.07 ‰) and the good replicability of the new method (as
307 shown by the error bars) demonstrate that this new method indeed allows the reliable and
308 quantitative recovery of both soluble and insoluble $S_{org}$.
309
310 *3.1.3. Suitability for multi-isotopes analyses*
311 In addition to the selective and quantitative recovery of different mineral (sulfates, sulfides
312 and $S^0$) and organic (solvent-extractable and non-extractable) S pools, the new stepwise
313 procedure developed allows the reliable determination of their S (multi-)isotope composition
314 by IRMS ($^{32}S$, $^{33}S$, $^{34}S$, $^{36}S$) or MC-ICPMS ($^{32}S$, $^{33}S$, $^{34}S$). In the present case, the S multi-
315 isotope composition of the investigated samples (from IRMS analysis of $SF_6$ gas) showed
316 mass-dependent fractionation of all S-isotopes with small but significant $\Delta^{33}S$ and $\Delta^{36}S$
317 values, within the range of $\Delta^{33}S \approx \pm 0.10$ ‰ and $\Delta^{36}S \approx \pm 1.50$ ‰ (Fig. 6 and Table 4) that are
318 expected for sediments younger than 2 Ga (see review by Johnston, 2011).
319
320 *3.1.4. Suitability for pure organic substrates*

The Rozel Point oil was primarily used here to test our oxidation procedure on 'pure' S-rich (> 90 mg S/g oil) organic matter. The $^{34}S$ composition of soluble $S_{org}$ as obtained from the new method ($\delta^{34}S$ = -6.05 ±0.11 ‰, Table 4) differed by ≈ 1.5 ‰ from the EA-IRMS measurement ($\delta^{34}S$ = -7.5 ±0.3 ‰). Still, most of $S_{org}$ could be recovered with the new method (with TS estimated to 9.18 ±0.1 % against 9.29 ±0.2 % with EA-IRMS), supporting the applicability of our procedure to 'pure' petroleum mixtures of OSC (possibly with a longer reaction time).

Yet, the efficiency of the method on fresh biological OSC and on very mature OSC (*e.g.*, Precambrian organic matter) remains to be established but should not be problematic.

## 3.2. Comparison with literature data and further interpretation of the geological record

Though the source rocks considered in this study have already been largely studied, the S stable (multi-)isotope composition of their different S pools remains poorly documented. A comparison between our $^{34}S$ data and those reported in previous studies of the Monterey and the Green River Formations is illustrated in Figure 7. This is complemented by data obtained for the present-day Lake Dziani Dzaha. Our multi-pool and multiple S-isotope data (Table 4), although still limited, were further used to bring new insights on our present understanding of the S isotope signatures observed in these settings (Fig. 8).

### *3.2.1. Monterey Formation*

The investigated sample of the Monterey Fm mainly contained sulfides and insoluble $S_{org}$ (4.73 ±0.30 and 3.57 ±0.22 mg/g of dry sediment, respectively; Table 4). Sulfates and soluble $S_{org}$ were also present but their concentrations were *ca*. ten times lower than those of sulfides and insoluble $S_{org}$, respectively (Table 4). $S^0$ was not detected, in accordance with the

literature (Zaback and Pratt, 1992). The presence of sulfates (which are only 2-4 ‰ $^{34}S$-enriched relative to sulfides; Table 4) was not described as primary in previous literature and could either correspond to artifactual oxidation products formed after sampling (likely during transport and storage) from sulfide minerals and potential organic polysulfides, or to secondary gypsum possibly derived from oxidation of S associated to migrating hydrocarbons (personal communication A.L. Sessions). Sulfides appeared 3-5 ‰ depleted in $^{34}S$ ($\delta^{34}S$ = +2.79 ±0.61 ‰) relative to soluble ($\delta^{34}S$ = +6.01 ±0.20 ‰) and insoluble ($\delta^{34}S$ = +8.73 ±0.04 ‰) $S_{org}$. This is consistent with literature data (Zaback & Pratt, 1992, Fig. 5) and with classical biogeochemical models of the S cycle in 'open' sedimentary systems (Fig. 8a).

Indeed, despite a large heterogeneity of sedimentary facies in the Monterey Fm, most of them are described as marine-influenced deposits (Orr, 1986; Zaback and Pratt, 1992). In these environments, S mainly derives from marine sulfates ($\delta^{34}S \approx +20$ ‰) which, in anoxic porewaters, can be reduced to $H_2S$ by MSR (Canfield and Des Marais, 1993). This major microbial process is associated with a large depletion in $^{34}S$, typically with $\delta^{34}S_{porewater\ sulfate}$ - $\delta^{34}S_{H2S}$ = 30 to 50 ‰ (Habicht and Canfield, 1997; Canfield, 2001). $^{34}S$-depleted $H_2S$ can then react with sedimentary iron or organic matter to produce iron sulfides or OSC, respectively. While the formation of iron sulfides only induces small S isotope fractionations, the sulfurization of organic matter seems to induce a slight $^{34}S$-enrichment (generally < 5 ‰) of $S_{org}$ relative to sulfides (Orr, 1986; Werne et al., 2003; Amrani, 2014). This is classically explained by a different timing of sulfurization, with the formation of iron sulfides (classically pyrite) occurring faster than the sulfurization of organic matter (Tuttle, 1991; Tuttle and Goldhaber, 1993; Werne et al., 2003). As schematized in Figure 8a, the delayed sulfurization of organic matter likely involves sulfates/reduced sulfur species enriched in $^{34}S$ by Rayleigh fractionation of the residual inorganic S pool. With time, this may result in a continuous enrichment of the $\delta^{34}S$ signatures of sulfides and $S_{org}$ until the source of mineral S is totally

depleted (Thode et al., 1961; Zaback and Pratt, 1992; Tuttle and Goldhaber, 1993; Fig 8a), as supported by the large range of $\delta^{34}S$ values of sulfides (between ≈ -9 ‰ and ≈ +20 ‰) reported for the Monterey Fm (Fig. 7; Zaback and Pratt, 1992). However, upon Rayleigh fractionation, one would predict positive $\Delta^{33}S$ (> 0.1 ‰) and strongly negative $\Delta^{36}S$ (< 1.0 ‰) (see Ono et al., 2006b; Sansjofre et al., 2016) which would result from mass-conservation effects (*e.g.* Farquhar et al., 2007). These values are however not observed in the present study, which deserves further investigation with a larger set of samples.

### *3.2.2. Green River Fm and Lake Dziani Dzaha*

As for the Monterey Fm, the main S pools in the selected samples from the Mahogany Zone of the Green River Fm and from the sub-surface sediments of Lake Dziani Dzaha were sulfides and $S_{org}$ (Table 4). This latter, however, essentially occurred as solvent insoluble $S_{org}$ in Lake Dziani Dzaha (0.34 ±0.05 and 3.69 ±0.18 mg/g of dry sediment for soluble and insoluble $S_{org}$, respectively), whereas the amount of soluble $S_{org}$ in the sample from the Green River Fm was of the same order of magnitude as insoluble $S_{org}$ (2.32 ±0.02 and 3.79 ±0.25 mg/g of dry sediment, respectively). Sulfides (essentially iron sulfides) were also present in a *ca.* four times higher concentration in the Green River Fm than in Lake Dziani. Variable relative abundances of the main S pools between both samples might reflect varying organic matter source or nature, sulfurization mechanisms, iron availability and depositional and diagenetic (e.g., ageing) histories (Table 2). A significant amount of $S^0$ (0.66 ±0.04 mg/g of dry sediment) was also detected in Lake Dziani Dzaha sediments while only traces (< 0.005 mg/g of dry sediment) were detected in the Green River sample. Low amounts of sulfates (< 5.5 % of total S) were recovered in both samples, which likely are artifactual oxidation products of mineral sulfides and eventual organic polysulfides. A strong argument for the absence of native sulfates in sediments from Lake Dziani Dzaha is the very low content of

sulfates (< 3 µM) in the present-day partially anoxic water column (Leboulanger et al., 2017) which is far from their supersaturation threshold. Despite differences in S content and speciation, the selected samples from the Green River Fm and from Lake Dziani showed striking similarities in their S multi-isotope compositions (Table 4 and Figure 7), with sulfides exceptionally enriched in heaviest S-isotopes (*i.e.*, $\delta^{34}S \approx +35$ ‰), while solvent soluble and insoluble $S_{org}$ being strongly depleted (by -25 to -30 ‰ for $^{34}S$) relative to sulfides (Table 4). Highly-$^{33}S$, $^{34}S$ and $^{36}S$-enriched $S^0$ was also observed in Lake Dziani Dzaha with values of $\delta^{34}S$, $\delta^{33}S$ and $\delta^{36}S$ slightly above those of sulfides (≈ +4, +2 and +7 ‰, respectively, *i.e.* ≈ +5.5 % of their values). Such uncommon S isotope features suggest strong similarities between these two ecosystems and a biogeochemical functioning clearly distinct from that of marine systems such as the Monterey Fm (Figs. 7 and 8).

$^{34}S$ highly-enriched sulfides have already been reported in samples from the late stages of the Green River Fm (Thode et al., 1958; Mauger et al., 1973; Tuttle and Goldhaber, 1993). The authors suggested that this enrichment was the result of a long-term Rayleigh fractionation process in past Green River lakes, driven by MSR and the diagenetic precipitation of depleted sulfides. According to Tuttle and Goldhaber (1993), a main difference with 'open' marine systems is that Green River lakes behaved as 'closed' systems, *i.e.* with no renewing of sulfate from the water column. Lake Dziani Dzaha can actually be considered similarly. This hypersaline tropical and insular stratified phreatomagmatic crater lake has no present-day connection to seawater, but its high S content most likely originates from initial marine sulfates (Leboulanger et al., 2017). In such 'closed' and stratified systems, the presence of a large anoxic water layer favors the production of sulfides by MSR and their subsequent precipitation as iron sulfides or their reaction with of organic matter, inducing a progressive enrichment in heavy isotopes of the residual S pool (Fig. 8b). It is noteworthy, however, that the geological record of the Green River Fm is the result of multiple long-scale sedimentary

421 evolutions over 100,000 years (Tuttle and Goldhaber, 1993), whereas the sedimentary story of
422 Lake Dziani Dzaha is less than 9000 years (Zinke et al., 2003). Different mechanisms could
423 have been involved in the temporal evolution of isotopic signature recorded in both systems.
424 Remarkably, as mentioned above, "closed"-system (Rayleigh-type) model predicts positive
425 $\Delta^{33}S$ and negative $\Delta^{36}S$ signatures which, again, were not observed here, possibly pointing
426 towards yet unkwnown specific S fractionation mechanisms.
427 The second remarkable feature observed for the Green River Fm and Lake Dziani Dzaha was
428 the strong depletion in heavy S isotopes of $S_{org}$ relative to sulfides (by -25 to -30 ‰ for $^{34}S$).
429 Such an isotopic shift has been previously reported in some studies of the Green River Fm,
430 but the values were not discussed further than the fact that they were out of range compared to
431 usual marine and euxinic environments (Mauger et al., 1973; Tuttle and Goldhaber, 1993).
432 Interestingly, a recent compound-specific $^{34}S/^{32}S$ analysis of organic matter from the Cariaco
433 Basin showed a *ca.* 10 ‰ depletion of several OSC (*e.g.*, triterpenoid thianes, and acyclic
434 isoprenoid thiophenes and thiolanes) relative to pyrite and to total extractable and residual $S_{org}$
435 (Raven et al., 2015). The authors suggested that total $S_{org}$ likely contains a mixture of OSC
436 with distinct S-isotopic compositions formed by different sulfurization pathways (reversible
437 vs irreversible sulfurization processes). Shawar et al. (2018) further suggested that $^{34}S$-
438 depletion of OSC relative to pyrite could be the result of competitive reactions between iron,
439 sulfur and organic matter, in particular in iron-limited environments. Under these specific
440 conditions, contrary to the 'open' marine systems described above, organic compounds might
441 react with reduced sulfur species at the earliest stage of burial more efficiently than iron, thus
442 recording the $\delta^{34}S$ signature of reactive sulfides whereas the formation of iron sulfides might
443 be delayed due to complexation or sorption of iron by the organic matter (Fig. 8b). S-isotopic
444 shifts between $S_{org}$ and mineral sulfides might thus result from a predominant kinetic isotope

445 effects occurring during the fast sulfurization of organic matter by different pathways that
446 remain to be characterized.
447
448 **4. CONCLUSIONS**
449 We validated a new stepwise chemical procedure for the quantitative recovery and multi-
450 isotope ($^{33}S$, $^{34}S$ and $^{36}S$) analysis of $S_{org}$ present in both solvent-extractable (bitumen) and
451 residual (kerogens) organic matter. This method is further compatible with the analysis of
452 different inorganic S species ($S^0$, sulfates and sulfides) in the same samples. The most
453 distinguishing feature of this procedure is the use of NaOCl as an oxidative agent for the
454 degradation of organic matter and release of $S_{org}$ as recoverable sulfates. The efficiency of this
455 analytical oxidation step was demonstrated with geological samples of various age and S-
456 content (contemporary anoxic sediment, source rocks and oil), noticeably showing that it does
457 not introduce any artificial fractionation of $S_{org}$ multi-isotopes. This method can be used either
458 for the determination by EA-IRMS of the S-content and $\delta^{34}S$ of different S-pools recovered as
459 $Ag_2S$ powders, or for the high-precision multi-isotope analysis of these $Ag_2S$ powders by
460 IRMS ($\delta^{33}S$, $\delta^{34}S$ and $\delta^{36}S$ from $SF_6$) or MC-ICPMS ($\delta^{33}S$, $\delta^{34}S$).
461 The application of this S multi-pool approach to samples from the Mahogany zone of the
462 Green River Fm and the contemporaneous Lake Dziani Dzaha revealed striking and similar
463 features of their S isotope composition, including highly-enriched mineral sulfides (with
464 values of $\delta^{34}S$ around +35‰), and pools of $S_{org}$ depleted in $^{34}S$ by *ca.* -27 ‰ relative to
465 sulfides. This depletion contrasts with the typical (+5/+10 ‰) enrichment in $^{34}S$ of $S_{org}$
466 relative to sulfides observed in marine sediments and confirmed in the present study with a
467 sample from the Monterey Fm (for which we report a +4.9 ‰ enrichment in $^{34}S$ of $S_{org}$
468 relative to sulfides). Such uncommon S isotopic characteristics probably point to fast

sulfurization of organic matter (with a kinetically controlled S fractionation) from $^{34}S$-enriched sulfides/sulfates, leading to a strong $^{34}S_{org}$ depletion.

**ACKNOWLEDGEMENTS**

The authors would like to thank Bryan Killingsworth (IPGP), Amaury Bouyon (IPGP), Laetitia Guibourdenche (IPGP) and François Fourel (LEHNA) for their precious suggestions and assistance in this work, as well as Alex L. Sessions and an anonymous reviewer who helped to improve the manuscript with their constructive feedback.

This study was funded by TOTAL E&P, the Lyon Institute of Origins (LabEx LIO) and the French CNRS interdisciplinary research program (ISOTOP 2018-2019, MULTISORG project).

**REFERENCES**

Adam, P., Schmid, J.C., Mycke, B., Strazielle, C., Connan, J., Huc, A., Riva, A., Albrecht, P., 1993. Structural investigation of nonpolar sulfur cross-linked macromolecules in petroleum. Geochim. Cosmochim. Acta 57, 3395–3419.

Albalat, E., Telouk, P., Balter, V., Fujii, T., Miossec, P., Zoulim, F., Puisieux, A., 2016. Sulfur isotope analysis by MC-ICP-MS and application to small medical samples. J. Anal. Atom.Spectrom. 31, 1002–1011.

Amrani, A., 2014. Organosulfur compounds: Molecular and isotopic evolution from biota to oil and gas. Annu. Rev. Earth Planet. Sci. 42, 733–768.

Amrani, A., Deev, A., Sessions, A.L., Tang, Y., Adkins, J.F., Hill, R.J., Moldowan, J.M., Wei, Z., 2012. The sulfur-isotopic compositions of benzothiophenes and dibenzothiophenes as a proxy for thermochemical sulfate reduction. Geochim.

493 Cosmochim. Acta 84, 152–164.

494 Amrani, A., Sessions, A.L., Adkins, J.F., 2009. Compound-specific δ34S analysis of volatile
495 organics by coupled GC/multicollector-ICPMS. Anal. Chem. 81, 9027–9034.

496 Anderson, T.F., Pratt, L.M., 1995. Isotopic evidence for the origin of organic sulfur and
497 elemental sulfur in marine sediments, in: Vairavamurthy, M., Schoonen, M.A.A. (Eds.),
498 Geochemical Transformations of Sedimentary Sulfur. pp. 378–396.

499 Arnold, G.L., Brunner, B., Müller, I.A., Røy, H., 2014. Modern applications for a total sulfur
500 reduction distillation method - what's old is new again. Geochem. Trans. 15, 1–12.

501 Au Yang, D., Landais, G., Assayag, N., Widory, D., Cartigny, P., 2016. Improved analysis of
502 micro- and nanomole-scale sulfur multi- isotope compositions by gas source isotope ratio
503 mass spectrometry. Rapid Commun. Mass Sp. 30, 897–907.

504 Bigeleisen, J., Mayer, M.G., 1947. Calculation of equilibrium constants for isotopic exchange
505 reactions. J. Chem. Phys. 15, 261–267.

506 Blumer, M., 1957. Removal of elemental sulfur from hydrocarbon fractions. Anal. Chem. 29,
507 1039–1041.

508 Bradley, W.H., 1964. Geology of Green River Formation and associated Eocene rocks in
509 south- western Wyoming and adjacent parts of Colorado and Utah. Geol. Surv. Prof.
510 Pap. 496-A, 81–84.

511 Canfield, D.E., 2001. Biogeochemistry of sulfur isotopes. Rev. Mineral. Geochem. 43, 607–
512 636.

513 Canfield, D.E., Boudreau, B.P., Mucci, A., Gundersen, J.K., 1998. The early diagenetic
514 formation of organic sulfur in the sediments of Mangrove Lake, Bermuda. Geochim.

515 Cosmochim. Acta 62, 767–781.

516 Canfield, D.E., Raiswell, R., Westrich, J.T., Reaves, C.M., Berner, R.A., 1986. The use of
517 chromium reduction in the analysis of reduced inorganic sulfur in sediments and shales.
518 Chem. Geol. 54, 249–254.

519 Eardley, A.J., 1963. Oil seeps at Rozel Point. Utah Geol. Mineral. Surv. Spec. Stud. 5.

520 Eschka, A., 1874. Estimation of sulphur in coal and coke. J. Chem. Soc. 27, 1007.

521 Farquhar, J., Bao, H., Thiemens, M., 2000. Atmospheric influence of Earth's earliest sulfur
522 cycle. Science 289, 756–758.

523 Farquhar, J., Johnston, D.T., Wing, B.A., Habicht, K.S., Canfield, D.E., Airieau, S.,
524 Thiemens, M.H., 2003. Multiple sulphur isotopic interpretations of biosynthetic
525 pathways: implications for biological signatures in the sulphur isotope record.
526 Geobiology 1, 27–36.

527 Farquhar, J., Wing, B.A., 2003. Multiple sulfur isotopes and the evolution of the atmosphere.
528 Earth Planet. Sc. Lett. 213, 1–13.

529 Farquhar, J., Johnston, D.T., Wing, B.A., 2007. Implications of conservation of mass effects
530 on mass-dependent isotope fractionations: Influence of network structure on sulfur
531 isotope phase space of dissimilatory sulfate reduction. Geochim. Cosmochim. Acta 71,
532 5862-5875.

533 Forrest, J., Newman, L., 1977. Silver-110 Microgram sulfate analysis for the short time
534 resolution of ambient levels of sulfur aerosol. Anal. Chem. 49, 1579–1584.

535 Fossing, H., Jorgensen, B.B., 1989. Measurement of bacterial sulfate reduction in sediments:
536 Evaluation of a single-step chromium reduction method. Biogeochemistry 8, 205–222.

Fourel F., Martineau F., Seris M. and Lécuyer C. 2014. Simultaneous N, C, S stable isotope analyses using new purge and trap technology. Rapid Commun. Mass Sp. 28, 2587–2594.

Giesemann, A., Jager, H., Norman, A.L., Krouse, H.R., Brand, W.A., 1994. On-line sulfur-isotope determination using an elemental analyzer coupled to a mass spectrometer. Anal. Chem. 66, 2816–2819.

Gröger, J., Franke, J., Hamer, K., Schulz, H.D., 2009. Quantitative recovery of elemental sulfur and improved selectivity in a chromium-reducible sulfur distillation. Geostand. Geoanal. Res. 33, 17–27.

Hulston, J. R., Thode, H. G., 1965. Cosmic ray produced 36S and 33S in metallic phase of iron meteorites: J. Geophys. Res. 70, 4435–4442.

Johnston, D.T., 2011. Multiple sulfur isotopes and the evolution of Earth ' s surface sulfur cycle. Earth-Sci. Rev. 106, 161–183.

Johnston, D.T., Farquhar, J., Wing, B.A., Kaufman, A.J., Canfield, D.E., Habicht, K.S., 2005. Multiple sulfur isotope fractionations in biological systems : a case study with sulfate reducers and sulfur disproportionators. Am. J. Sci. 305, 645–660.

Kutuzov, I., Rosenberg, Y.O., Bishop, A., Amrani, A., 2018. The Origin of Organic Sulphur Compounds and Their Impact on the Paleoenvironmental Record. In: H. Wilkes (ed.), Hydrocarbons, Oils and Lipids: Diversity, Origin, Chemistry and Fate. Handbook of Hydrocarbon and Lipid Microbiology. Springer, Cham.

Labidi, J., Farquhar, J., Alexander, C.M.O'D., Eldridge, D.L., Oduro, H., 2017. Mass independent sulfur isotope signatures in CMs : Implications for sulfur chemistry in the early solar system. Geochim. Cosmochim. Acta 196, 326-350.

560 Leboulanger, C., Agogué, H., Bernard, C., Bouvy, M., Carré, C., Cellamare, M., Duval, C.,
561 Fouilland, E., Got, P., Intertaglia, L., Lavergne, C., Le Floc'h, E., Roques, C., Sarazin,
562 G., 2017. Microbial diversity and cyanobacterial production in Dziani Dzaha crater lake,
563 a unique tropical thalassohaline environment. PLoS One 12, 1–28.

564 Li, W., Cho, E.H., 2005. Coal desulfurization with sodium hypochlorite. Energ. Fuel 19, 499–
565 507.

566 Luo, G., Richoz, S., van de Schootbrugge, B., Algeo, J., Xie, S., Ono, S., Summons, R.E.,
567 2018. Multiple sulfur-isotopic evidence for a shallowly stratified ocean following the
568 Triassic-Jurassic boudary mass-extinction. Geochim. Cosmochim. Acta 231, 73–87.

569 Mauger, R.L., Kayser, R.B., Gwynn, W., 1973. A Sulfur isotopic study of Uinta Basin
570 hydrocarbons. Utah Geol. Mineral. Surv. Spec. Ser. 41, 19.

571 Milesi, V.P., Debure, M., Marty, N.C.M., Capano, M., Jezequel, D., Steefel, C.I., Rouchon,
572 V., Albéric, P., Bard, E., Sarazin, G., Guyot, F., Virgone, A., Gaucher, E.C., Ader, M.,
573 2020. Early Diagenesis of Lacustrine Carbonates in Volcanic Settings: The Role of
574 Magmatic $CO_2$ (Lake Dziani Dzaha, Mayotte, Indian Ocean). ACS Earth Space Chem.,
575 4, 363-378.

576 Oduro, H., Kamyshny, A., Guo, W., Farquhar, J., 2011. Multiple sulfur isotope analysis of
577 volatile organic sulfur compounds and their sulfonium precursors in coastal marine
578 environments. Mar. Chem. 124, 78–89.

579 Ono, S., Shanks, W.C., Rouxel, O.J., Rumble, D., 2007. S-33 constraints on the seawater
580 sulfate contribution in modern seafloor hydrothermal vent sulfides. Geochim.
581 Cosmochim. Acta 71, 1170–1182.

582 Ono, S., Wing, B., Johnston, D., Farquhar, J., Rumble, D., 2006a. Mass-dependent

583 fractionation of quadruple stable sulfur isotope system as a new tracer of sulfur
584 biogeochemical cycles. Geochim. Cosmochim. Acta 70, 2238–2252.

585 Ono, S., Wing, B., Rumble, D., Farquhar, J., 2006b. High precision anlysis of all four stable
586 isotopes of sulfur ($^{32}S$, $^{33}S$, $^{34}S$ and $^{36}S$) at nanomole levels using a laser fluorination
587 isotope-ratio-monitoring gas chromatography-mass spectrometry. Chem. Geol. 225, 30-
588 39.

589 Orr, W.L., 1986. Kerogen/asphaltene/sulfur relationships in sulfur-rich Monterey oils. Org.
590 Geochem.10, 499–516.

591 Paris, G., Sessions, A.L., Subhas, A.V., Adkins, J.F., 2013. MC-ICP-MS measurement of $\delta^{34}S$
592 and $\Delta^{33}S$ in small amounts of dissolved sulfate. Chem. Geol. 345, 50-61.

593 Passier, H.F., Middelburg, J.J., de Lange, G.J., Böttcher, M.E., 1999. Modes of sapropel
594 formation in the eastern Mediterranean : some constraints based on pyrite properties.
595 Marine Geology 153, 199-219.

596 Pepkowitz, L.P., Shirley, E.L., 1950. Microdetection of Sulfur. Anal. Chem. 23, 1709–1710.

597 Philippot, P., Van Zuilen, M., Lepot, K., Thomazo, C., Farquhar, J., Van Kranendonk, M.J.,
598 2007. Early Archaean Microorganisms Preferred Elemental Sulfur, Not Sulfate. Science
599 317, 1534-1537.

600 Raven, M.R., Adkins, J.F., Werne, J.P., Lyons, T.W., Sessions, A.L., 2015. Sulfur isotopic
601 composition of individual organic compounds from Cariaco Basin sediments. Org.
602 Geochem. 80, 53–59.

603 Raven, M.R., Fike, D.A., Gomes, M.L., Webb, S.M., Bradley, A.S., 2018. Organic carbon
604 burial during OAE2 driven by changes in the locus of organic matter sulfurization. Nat.

Commun. 9, 3409.

Raven, M.R., Sessions, A.L., Adkins, J.F., Thunell, R.C., 2016a. Rapid organic matter sulfurization in sinking particles from the Cariaco Basin water column. Geochim. Cosmochim. Acta 190, 175–190.

Raven, M.R., Sessions, A.L., Fischer, W.W., Adkins, J.F., 2016b. Sedimentary pyrite δ34S differs from porewater sulfide in Santa Barbara Basin: Proposed role of organic sulfur. Geochim. Cosmochim. Acta 186, 120–134.

Rees, C.E., 1978. Sulphur isotope measurements using SO2 and SF6. Geochim. Cosmochim. Acta 42, 383–389.

Sansjofre, P., Cartigny, P., Trindade, R.I.F., Nogueira, A.C.R., Agrinier, P., Ader, M., 2016. Multiple sulfur isotope evidence for massive oceanic sulfate depletion in the aftermath of Snowball Earth. Nat. Commun. 7, 12192.

Selvig, W.A., Fieldner, A.C., 1927. Sulfur in coal and coke: Check determinations by the Eschka, bomb-washing and sodium peroxide fusion methods. Ind. Eng. Chem. 19, 729–733.

Shawar, L., Halevy, I., Said-Ahmad, W., Feinstein, S., Boyko, V., Kamyshny, A., Amrani, A., 2018. Dynamics of pyrite formation and organic matter sulfurization in organic-rich carbonate sediments. Geochim. Cosmochim. Acta 241, 219–239.

Shawar, L., Said-Ahmad, W., Ellis, G.S., Amrani, A., 2020. Sulfur isotope composition of individual compounds in immature organic-rich rocks and possible geochemical implications. Geochim. Cosmochim. Acta, doi: 10.1016/j.gca.2020.01.034.

Siedenberg, K., Strauss, H., Podlaha, O., van den Boorn, S., 2018. Multiple sulfur isotopes

627 (δ34S, Δ33S) of organic sulfur and pyrite from Late Cretaceous to Early Eocene oil
628 shales in Jordan. Org. Geochem. 125, 29–40.

629 Sinninghe Damsté, J.S., Rijpstra, W.I.C., Kock-Van Dalen, A.C., De Leeuw, J.W., Schenck,
630 P.A., 1989. Quenching of labile functionalised lipids by inorganic sulphur species:
631 Evidence for the formation of sedimentary organic sulphur compounds at the early stages
632 of diagenesis. Geochim. Cosmochim. Acta 53, 1343–1355.

633 Smith, M.E., Carroll, A.R., 2015. Stratigraphy and Paleolimnology of the Green River
634 Formation, Western USA. Springer, Dordrecht.

635 Thode, H.G., Monster, J., Dunford, H.B., 1961. Sulphur isotope geochemistry. Geochim.
636 Cosmochim. Acta 25, 159–174.

637 Thode, H.G., Monster, J., Dunford, H.B., 1958. Sulphur isotope abundances in petroleum and
638 associated materials. Bulltetin Am. Assoc. Pet. Geol. 42, 2619–2641.

639 Thode, H.G., Rees, C.E., 1971. Measurement of sulphur concentrations and the isotope ratios
640 33S/32S, 34S/32S and 36S/32S in Apollo 12 samples. Earth Planet. Sci. Lett. 12, 434–
641 438.

642 Thomassot, E., Cartigny, P., Harris, J.W., Lorand, J.P., Rollion-Bard, C., Chaussidon, M.,
643 2009. Metasomatic diamond growth: A multi-isotope study (13C, 15N, 33S, 34S) of
644 sulphide inclusions and their host diamonds from Jwaneng (Botswana). Earth Planet. Sci.
645 Lett. 282, 79–90.

646 Tissot, B.P., Welte, D.H., 1984. Petroleum Formation and Occurrence, Second Edi. ed.
647 Springer-Verlag.

648 Tuttle, M.L., 1991. Geochemical, biogeochemical, and sedimentological studies of the Green

River Formation, Wyoming, Utah, and Colorado. USGS Numbered Ser. 1973-A-G, 200.

Tuttle, M.L., Goldhaber, M.B., 1993. Sedimentary sulfur geochemistry of the Paleogene Green River Formation, western USA: Implications for interpreting depositional and diagenetic processes in saline alkaline lakes. Geochim. Cosmochim. Acta 57, 3023–3039.

Wang, YG, Wei, X.Y., Yan, H.L., Liu, F.J., Li, P., Zong, Z.M., 2014. Sequential oxidation of Jincheng No. 15 anthracite with aqueous sodium hypochlorite. Fuel Process. Technol. 125, 182-189.

Werne, J.P., Lyons, T.W., Hollander, D.J., Formolo, M.J., Sinninghe Damsté, J.S., 2003. Reduced sulfur in euxinic sediments of the Cariaco Basin: sulfur isotope constraints on organic sulfur formation. Chem. Geol. 195, 159–179.

Werne, J.P., Lyons, T.W., Hollander, D.J., Schouten, S., Hopmans, E.C., Sinninghe Damsté, J.S., 2008. Investigating pathways of diagenetic organic matter sulfurization using compound-specific sulfur isotope analysis. Geochim. Cosmochim. Acta 72, 3489–3502.

Whitehouse, M.J., 2012. Multiple sulfur isotope determination by SIMS: Evaluation of reference sulfides for Δ33S with observations and a case study on the determination of Δ36S. Geostand. Geoanal.Res. 37, 19–33.

Young, E.D., Galy, A., Nagahara, H., 2002. Kinetic and equilibrium mass-dependent isotope fractionation laws in nature and their geochemical and cosmochemical significance. Geochim. Cosmochim. Acta 66, 1095–1104.

Zaback, D.A., Pratt, L.M., 1992. Isotopic composition and speciation of sulfur in the Miocene Monterey Formation : Reevaluation of sulfur reactions during early diagenesis in marine environments. Geochim. Cosmochim. Acta 56, 763–774.

672 Zinke, J., Reijmer, J.J.G., Thomassin, B.A., 2003. Systems tracts sedimentology in the lagoon
673 of Mayotte associated with the Holocene transgression. Sed. Geol. 160, 57-784.

**Table 1** Methods previously used for studying the $^{34}S$ composition of organic and mineral S. For further details about STRIP and $CrCl_2$ distillations, see 3.2. * Studies in which $^{33}S$ and/or $^{36}S$ were also measured. n/i: not investigated.

**Table 2** Origin, nature and use of samples. O = oxidation tests (Figs. 3 and 4), N = Raney nickel tests (Table 3), W = complete workflow procedure (triplicate analyses, Table 4), L = comparison with literature data and biogeochemical interpretation.

**Table 3** Comparison of $S_{org}$ contents (mg/g of dry sediment) released with the Raney nickel method (Oduro et al., 2011) and the new method from selected samples. TLE = solvent-soluble organic matter.

**Table 4** S content (mg/g of dry sediment) and multiple-isotope composition (‰ vs CDT) of the different S pools from the investigated samples. n/d: non determined or excluded value, due to either a lack of material (under limit of detection) or mass spectrometry issues/contaminations. *The $4^{th}$ replicate of Lake Dziani Dzaha was sampled in a different part of the core than the three others. It was therefore not used in the mass balance calculations. TLE $S_{org}$ = solvent-soluble $S_{org}$ and Kerogen $S_{org}$ = solvent-insoluble $S_{org}$.

Table 1

| Study | Sample type | Total S | Sulfides | Sulfates | $S^0$ | $S_{org}$ |
|---|---|---|---|---|---|---|
| Thode et al. (1958) | Oil | Calculated | Bubbled out | Centrifuged out | n/i | $Br_2$, HNO3 oxidation to sulfates, STRIP distillation, $SO_2$ IRMS |
| | Bulk sediment | n/i | $Br_2$, $HNO_3$ oxidation to sulfates, STRIP distillation, $SO_2$ IRMS | Dissolution + precipitation, STRIP distillation, $SO_2$ IRMS | n/i | n/i |
| Mauger et al. (1973) | Organic extract from tar sand | n/i | n/i | n/i | n/i | $Br_2$ oxidation + STRIP distillation, $SO_2$ IRMS |
| Orr (1986) | Solvent-extracted sediment | Calculated | $HNO_3$ oxidation to sulfates, EA-IRMS | n/i | n/i | Parr bomb oxidation to sulfates, EA-IRMS |
| | Oil/organic extract from sediment | | | | | Parr bomb oxidation to sulfates, EA-IRMS |
| Zaback and Pratt (1992) | Solvent-extracted sediment | Calculated | $CrCl_2$ distillation, $SO_2$ IRMS | Dissolution + precipitation, $SO_2$ IRMS | | |
| | Organic extract from the sediment | Calculated | | | Combustion, $SO_2$ IRMS | Parr bomb oxidation, $SO_2$ IRMS |
| Tuttle and Goldhaber (1993) | Bulk sediment | Calculated | $CrCl_2$ distillation, $SO_2$ IRMS analysis | $SO_2$ IRMS analysis | n/i | Eschka oxidation, $SO_2$ IRMS |
| Werne et al. (2008, 2003) | Solvent-extracted sediment | EA-IRMS on bulk sediment | $CrCl_2$ distillation, EA-IRMS | EA-IRMS on pore water precipitates | n/i | EA-IRMS |
| | Organic extract from the sediment | | $CrCl_2$ distillation, EA-IRMS | | n/i | EA-IRMS + compound-specific EA-IRMS |
| Amrani et al. (2012, 2009) | Oil/Organosulfur standard | EA-IRMS | n/i | n/i | n/i | Compound-specific MC-ICPMS |
| Oduro et al. (2011) | Solvent-extracted sediment | Calculated | $CrCl_2$ distillation, $SF_6$ IRMS* | STRIP distillation, $SF_6$ IRMS* on pore water precipitates | | n/i |
| | Organic extract from the sediment | Calculated | | | $CrCl_2$ distillation, $SF_6$ IRMS* | Raney Ni desulfurization + $CrCl_2$ distillation, $SF_6$ IRMS* |
| Raven et al. (2018, 2016a, 2016b, 2015) | Solvent-extracted sediment | Calculated | $HNO_3$ oxidation to sulfates, ion chromatography, ICPMS/EA-IRMS | Dissolution + precipitation, ion chromatography, ICPMS/EA-IRMS | | n/i |
| | Organic extract from the sediment | Calculated | | | Oxidation, ion chromatography, ICPMS/EA-IRMS | $H_2O_2$ oxidation, ion chromatography, ICPMS/EA-IRMS + compound-specific MC-ICPMS |
| Siedenberg et al. (2018) | Solvent-extracted sediment | n/i | $CrCl_2$ distillation, $SF_6$ IRMS* | n/i | | Eschka powder oxidation + STRIP distillation, $SF_6$ IRMS* |
| | Organic extract from the sediment | n/i | | | n/i | Eschka powder oxidation + STRIP distillation, $SF_6$ IRMS* |
| This study | Solvent-extracted sediment | EA-IRMS on bulk sediment | $CrCl_2$ distillation, $SF_6$ IRMS* | STRIP distillation, $SF_6$ IRMS* | | NaHClO oxidation + STRIP distillation, $SF_6$ IRMS* |
| | Oil/Organic extracts from the sediment | | | | $CrCl_2$ distillation, $SF_6$ IRMS* | NaHClO oxidation + STRIP distillation, $SF_6$ IRMS* |

Table 2

| | *Sample source* | *Sediment type* | *Age* | *TOC (%)* | *Use* |
|---|---|---|---|---|---|
| Lake Dziani Dzaha (Mayotte, Indian Ocean) | Sub-superficial sediment | Euxinic lake sediment | Modern (0-1 kyr after Milesi et al., 2020) | 9.2 ±0.3 | O + N + W + L |
| Green River Fm (UT, USA) | Outcrop & core sediments | Microbialite | Eocene (ca. 50 Myr) | 31.8 ±0.4 | O + N + W + L |
| Monterey Fm (CA, USA) | Outcrop sediment | Shale | Miocene (5-17 Myr) | 7.1 ±0.5 | O + W + L |
| Rozel Point oil (UT, USA) | Oil seep | Crude oil | Tertiary | 49.3 ±0.5 | O + N + W |
| Limagne Basin (Massif Central, France) | Outcrop sediment | Microbialite | Oligo-Miocene (5-34 Myr) | 13.4 ±0.1 | N |

Table 3

| | *New method* | *Raney nickel* |
|---|---|---|
| Lake Dziani Dzaha TLE | 0. 33 ± 0.05 (n=3) | 0.047 ± 0.01 (n=3) |
| Green River Fm TLE | 2.32 ± 0.02 (n=2) | 0. 11 ± 0.05 (n=2) |
| Limagne Basin kerogen | 1.11 ± 0.03 (n=2) | 0.32 ± 0.02 (n=2) |
| Rozel Point oil | 91.78 ± 1.05 (n=3) | 0.46 ± 0.12 (n=2) |

Table 4

| *Sample* | *Pool* | *Replicate* | *S quantity* | $\delta^{34}S$ | $\delta^{33}S$ | $\delta^{36}S$ | $\Delta^{33}S$ | $\Delta^{36}S$ |
|---|---|---|---|---|---|---|---|---|
| Monterey Fm | Sulfides | 1 | 4.759 | 2.666 | 1.465 | 5.67 | 0.028 | -0.53 |
| | | 2 | 5.015 | 2.251 | 1.252 | 4.89 | 0.029 | -0.51 |
| | | 3 | 4.416 | 3.454 | 1.874 | 7.16 | 0.032 | -0.53 |
| | Sulfates | 1 | 0.560 | 4.739 | 2.573 | 9.22 | 0.070 | -0.89 |
| | | 2 | 0.534 | 5.868 | 3.126 | 11.47 | 0.043 | -0.790 |
| | | 3 | 0.642 | 7.370 | 3.920 | 14.29 | 0.065 | -0.84 |
| | $S^0$ | 1 | < 0.005 | n/d | n/d | n/d | n/d | n/d |
| | | 2 | < 0.005 | n/d | n/d | n/d | n/d | n/d |
| | | 3 | < 0.005 | n/d | n/d | n/d | n/d | n/d |
| | Kerogen $S_{org}$ | 1 | 3.428 | 8.768 | 4.623 | 17.20 | 0.051 | -0.60 |
| | | 2 | 3.462 | 8.691 | 4.586 | 16.97 | 0.055 | -0.68 |
| | | 3 | 3.829 | 8.732 | 4.615 | 17.02 | 0.062 | -0.71 |
| | TLE $S_{org}$ | 1 | 0.339 | 5.871 | 3.145 | 11.62 | 0.061 | -0.65 |
| | | 2 | 0.269 | n/d | n/d | n/d | n/d | n/d |
| | | 3 | 0.285 | 6.151 | 3.295 | 11.86 | 0.067 | -0.94 |
| Rozel Point | Sulfides | 1 | < 0.005 | n/d | n/d | n/d | n/d | n/d |
| | | 2 | < 0.005 | n/d | n/d | n/d | n/d | n/d |
| | | 3 | < 0.005 | n/d | n/d | n/d | n/d | n/d |
| | Sulfates | 1 | < 0.005 | n/d | n/d | n/d | n/d | n/d |
| | | 2 | < 0.005 | n/d | n/d | n/d | n/d | n/d |
| | | 3 | < 0.005 | n/d | n/d | n/d | n/d | n/d |
| | $S^0$ | 1 | < 0.005 | n/d | n/d | n/d | n/d | n/d |
| | | 2 | < 0.005 | n/d | n/d | n/d | n/d | n/d |
| | | 3 | < 0.005 | n/d | n/d | n/d | n/d | n/d |
| | Kerogen $S_{org}$ | 1 | < 0.005 | n/d | n/d | n/d | n/d | n/d |
| | | 2 | < 0.005 | n/d | n/d | n/d | n/d | n/d |
| | | 3 | < 0.005 | n/d | n/d | n/d | n/d | n/d |
| | TLE $S_{org}$ | 1 | 92.836 | -6.165 | -3.034 | -11.58 | 0.081 | -1.07 |
| | | 2 | 90.728 | -6.025 | -2.963 | -11.33 | 0.079 | -1.08 |
| | | 3 | 91.765 | -5.960 | -2.924 | -11.18 | 0.085 | -1.06 |
| Lake Dziani | Sulfides | 1 | 2.363 | 35.143 | 18.027 | 69.07 | 0.014 | 0.37 |
| | | 2 | 2.485 | 35.651 | 18.278 | 69.86 | 0.008 | 0.17 |
| | | 3 | 2.382 | 35.528 | 18.216 | 70.14 | 0.009 | 0.67 |
| | | 4* | 2.522 | 37.126 | 19.027 | 72.71 | 0.011 | 0.14 |
| | Sulfates | 1 | 0.353 | n/d | n/d | n/d | n/d | n/d |
| | | 2 | 0.409 | n/d | n/d | n/d | n/d | n/d |
| | | 3 | 0.484 | n/d | n/d | n/d | n/d | n/d |
| | | 4* | 0.387 | 33.216 | 17.077 | 64.86 | 0.040 | -0.08 |
| | $S^0$ | 1 | 0.647 | n/d | n/d | n/d | n/d | n/d |
| | | 2 | 0.632 | n/d | n/d | n/d | n/d | n/d |
| | | 3 | 0.709 | n/d | n/d | n/d | n/d | n/d |
| | | 4* | 0.556 | 39.583 | 20.245 | 77.67 | -0.014 | 0.29 |
| | Kerogen $S_{org}$ | 1 | 3.768 | 6.701 | 3.491 | 13.82 | -0.019 | -0.06 |
| | | 2 | 3.478 | 5.933 | 3.119 | 12.05 | 0.003 | -0.35 |
| | | 3 | 3.812 | 6.781 | 3.546 | 14.05 | -0.006 | 0.02 |
| | | 4* | 3.603 | 8.228 | 4.290 | 16.69 | -0.004 | -0.09 |
| | TLE $S_{org}$ | 1 | 0.300 | 9.613 | 5.001 | 19.64 | -0.003 | 0.21 |
| | | 2 | 0.385 | 10.169 | 5.277 | 20.80 | -0.012 | 0.30 |
| | | 3 | 0.319 | 10.548 | 5.474 | 21.56 | -0.010 | 0.34 |
| | | 4* | 0.256 | 9.070 | 4.705 | 18.17 | -0.020 | -0.21 |
| Green Riv. Fm | Sulfides | 1 | 10.002 | 34.714 | 17.733 | 68.98 | -0.062 | 1.08 |
| | | 2 | 9.960 | 35.337 | 18.050 | 69.98 | -0.061 | 0.88 |
| | | 3 | 9.303 | 35.266 | 17.999 | 69.78 | -0.076 | 0.82 |
| | Sulfates | 1 | 0.905 | 27.832 | 14.248 | n/d | -0.055 | n/d |
| | | 2 | < 0.005 | n/d | n/d | n/d | n/d | n/d |
| | | 3 | 0.924 | 25.349 | 12.971 | n/d | -0.070 | n/d |
| | $S^0$ | 1 | < 0.005 | n/d | n/d | n/d | n/d | n/d |
| | | 2 | < 0.005 | n/d | n/d | n/d | n/d | n/d |
| | | 3 | < 0.005 | n/d | n/d | n/d | n/d | n/d |
| | Kerogen $S_{org}$ | 1 | 3.821 | 9.002 | 4.644 | n/d | -0.047 | n/d |
| | | 2 | 4.013 | 8.690 | 4.497 | 17.78 | -0.034 | 0.11 |
| | | 3 | 3.527 | 10.069 | 5.209 | n/d | -0.029 | n/d |
| | TLE $S_{org}$ | 1 | 2.302 | 5.848 | 3.062 | 12.03 | -0.010 | -0.22 |
| | | 2 | < 0.005 | n/d | n/d | n/d | n/d | n/d |
| | | 3 | 2.331 | 5.718 | 3.001 | 12.98 | -0.005 | 0.94 |

**Fig. 1.** Proposed workflow for the sequential recovery of organic and mineral S from sediments/oils as $Ag_2S$ powders, prior to their fluorination and S multi-isotope analysis.

**Fig. 2.** Experimental setup used for S distillation; **a**, sample with gentle reflux, **b**, reducing solution ($CrCl_2$/STRIP), **c**, nitrogen flush, **d**, water acid-trap, **e**, silver nitrate sulfur-trap.

**Fig. 3.** Organic carbon content (**a**) and $S_{org}$ recovery (**b**) of selected samples along 48 hours of NaOCl oxidation at 60°C.

**Fig. 4.** $\delta^{34}S$ of recovered $S_{org}$ as a function of NaOCl oxidation time at 60°C.

**Fig. 5.** Comparison of S mass balances between bulk EA-IRMS and multi-pool $SF_6$-IRMS (new method) analyses; **a**, TS content calculated from $Ag_2S$ weighing as a function of EA-IRMS bulk evaluation; **b**, bulk $\delta^{34}S$ calculated with mass-balance equations from multi-pool $SF_6$-IRMS analyses, as a function of EA-IRMS bulk evaluation. Error bars show the standard deviation between triplicate analyses.

**Fig. 6.** Multi-isotope data from the samples of this study; open diamonds, sulfides, open circles, sulfates, open triangles, $S^0$, black diamonds, soluble $S_{org}$, black circles, insoluble $S_{org}$. **a** and **c** show mass-dependent fractionation of all S-isotopes. **b** and **d** show the interest of the Δ notation to enhance the variability between samples.

**Fig. 7.** Comparison between $\delta^{34}S$ in sedimentary sulfides and kerogens. Data for the Green River Fm is from Tuttle & Goldhaber (1993), data for the Monterey Fm is from Zaback and Pratt (1992). The expected range for marine sediments is extrapolated after Orr (1986).

**Fig. 8.** Two possible models for S geochemistry and organic matter sulfurization during sediment deposition and diagenesis. **A** shows S fractionation associated with organic matter sulfurization in the anoxic part of the sediments in 'open' marine environments such as the Monterey Fm. The inflow S derives from marine sulfates. **B** shows S fractionation associated with organic matter sulfurization in a partially sulfidic stratified water column with a high $H_2S$/sulfates ratio from a 'closed' system such as some Green River Fm members and Lake Dziani Dzaha. The inflow S derives from enriched sulfates resulting from the Rayleigh fractionation of marine sulfates in a closed system (as suggested by Tuttle, 1991). MSR = Microbial Sulfate Reduction.

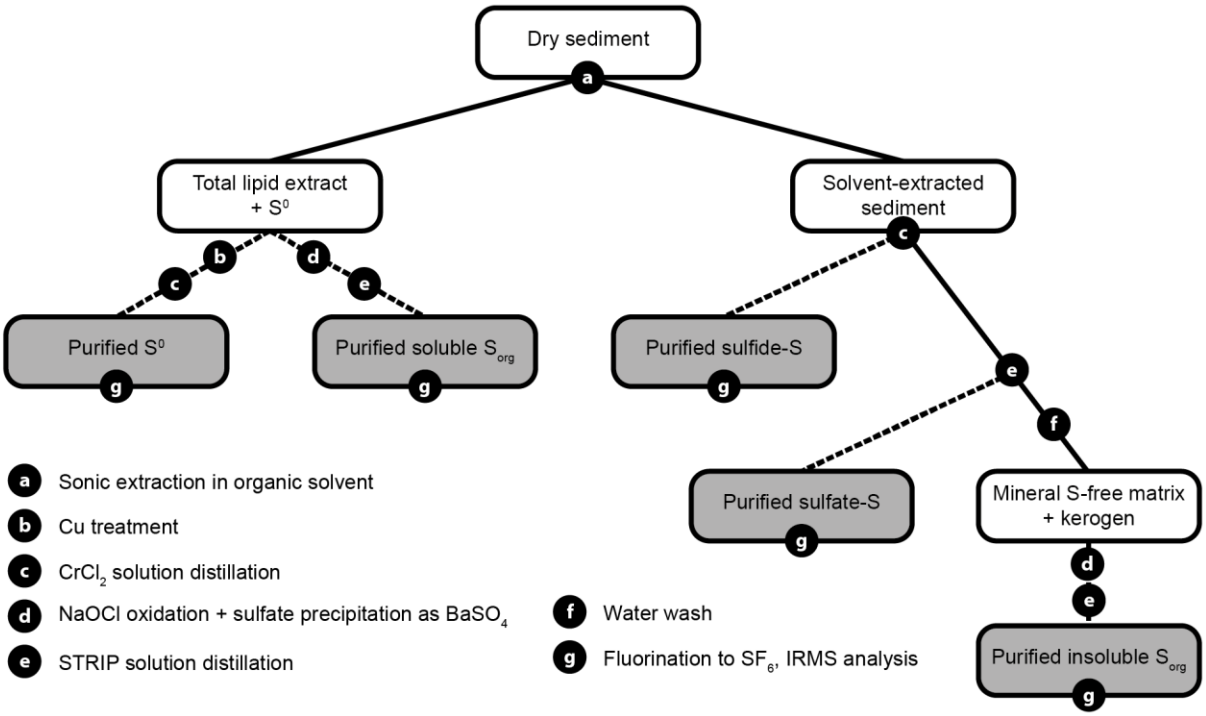
Dry sediment
a
Total lipid extract + S0
Solvent-extracted sediment
b
c
d
e
c
Purified S0
Purified soluble Sorg
Purified sulfide-S
g
g
g
e
f
Purified sulfate-S
Mineral S-free matrix + kerogen
d
e
Purified insoluble Sorg
g
a Sonic extraction in organic solvent
b Cu treatment
c CrCl2 solution distillation
d NaOCl oxidation + sulfate precipitation as BaSO4
e STRIP solution distillation
f Water wash
g Fluorination to SF6, IRMS analysis

Figure 1

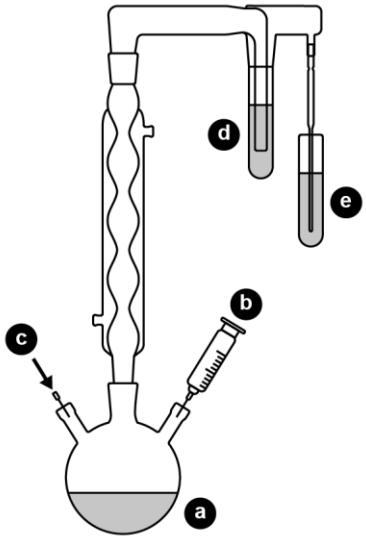


Figure 2

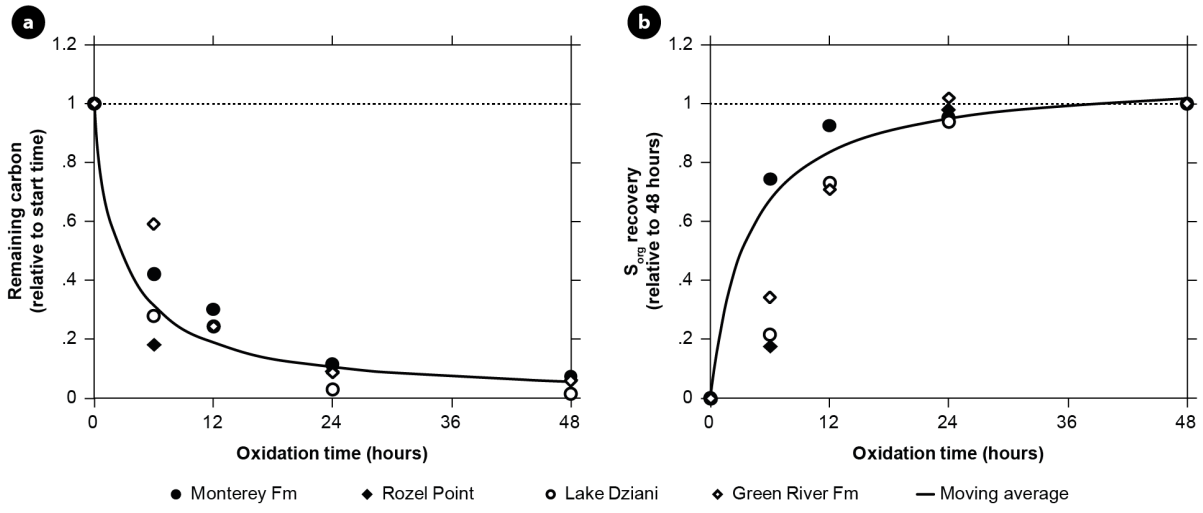
a
b
Remaining carbon
(relative to start time)
$S_{org}$ recovery
(relative to 48 hours)
1.2
1
.8
.6
.4
.2
0
0
12
24
36
48
Oxidation time (hours)
Monterey Fm
Rozel Point
Lake Dziani
Green River Fm
Moving average

Figure 3

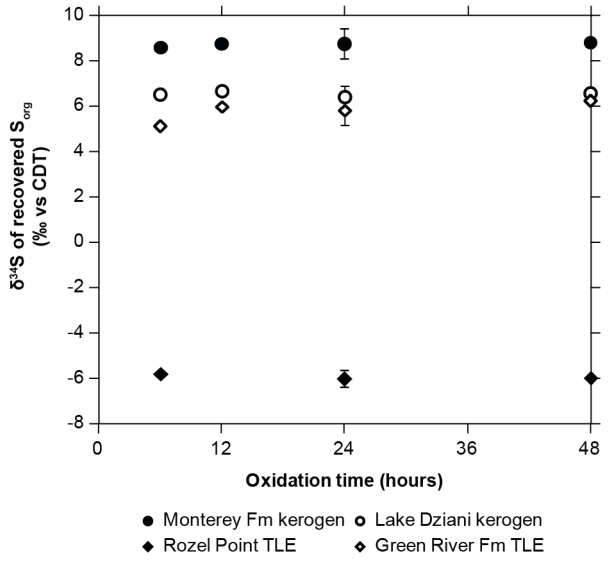
10
8
6
4
2
0
-2
-4
-6
-8
0
12
24
36
48
δ34S of recovered Sorg
(‰ vs CDT)
Oxidation time (hours)
Monterey Fm kerogen
Lake Dziani kerogen
Rozel Point TLE
Green River Fm TLE

Figure 4

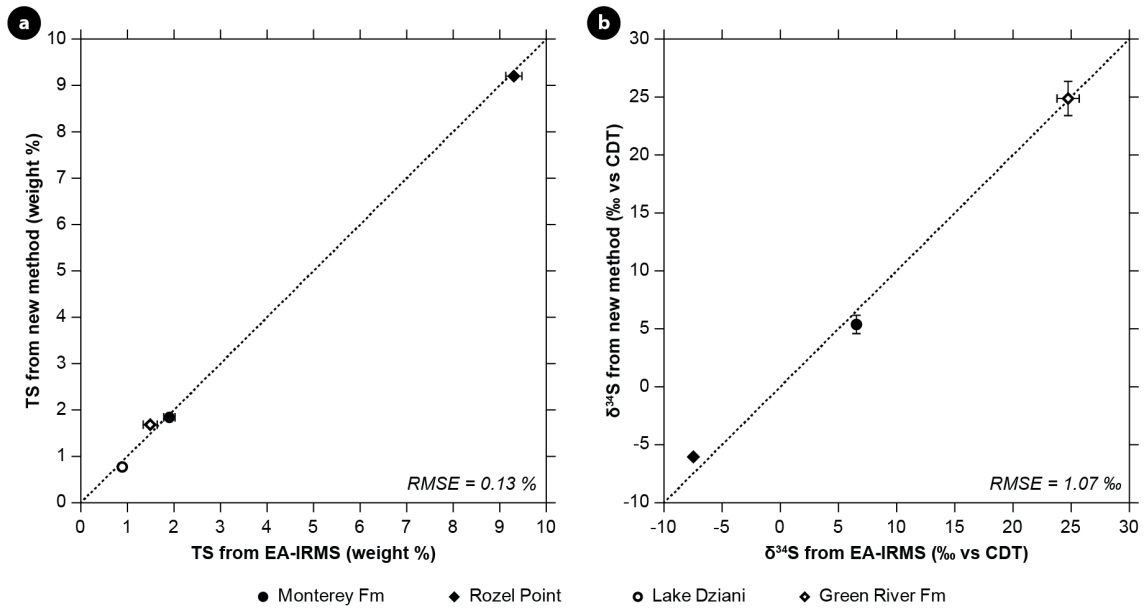
a
TS from new method (weight %)
TS from EA-IRMS (weight %)
RMSE = 0.13 %
b
δ³⁴S from new method (‰ vs CDT)
δ³⁴S from EA-IRMS (‰ vs CDT)
RMSE = 1.07 ‰
Monterey Fm
Rozel Point
Lake Dziani
Green River Fm

Figure 5

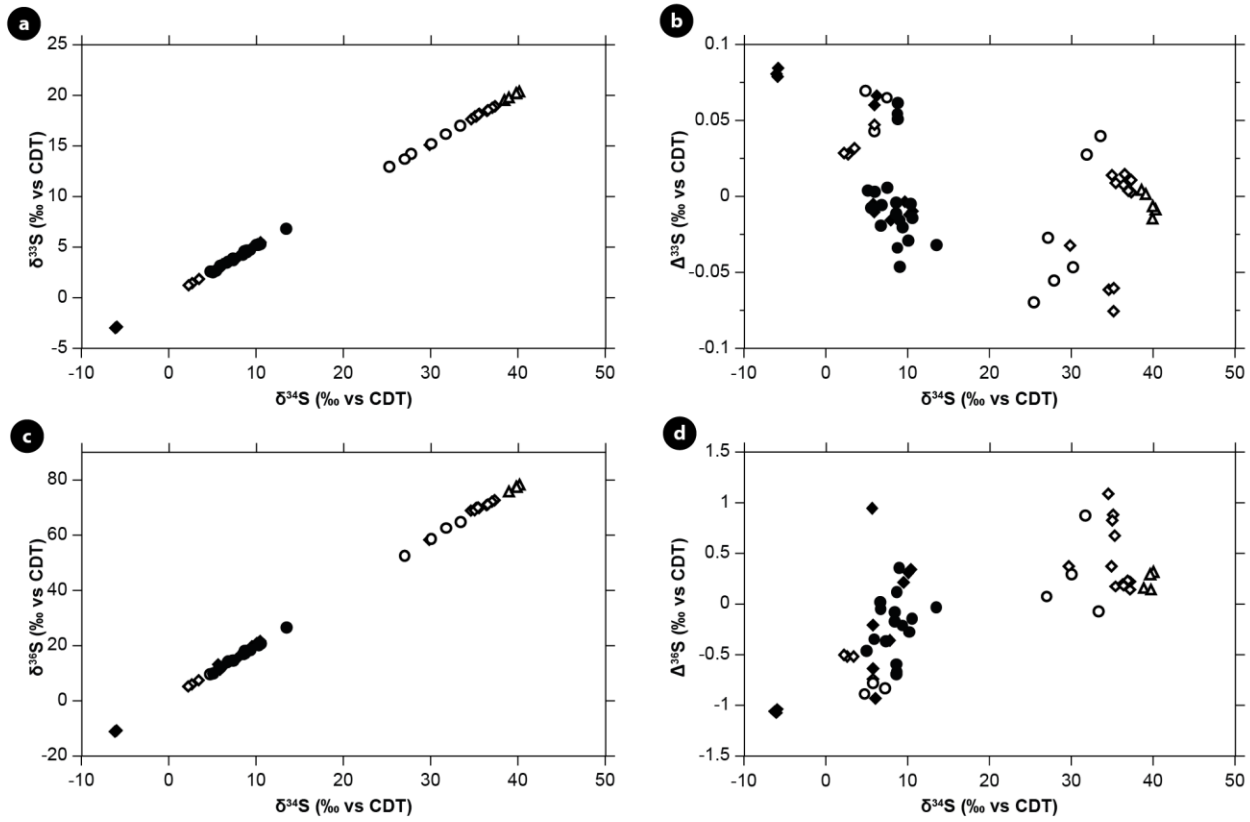


Figure 6

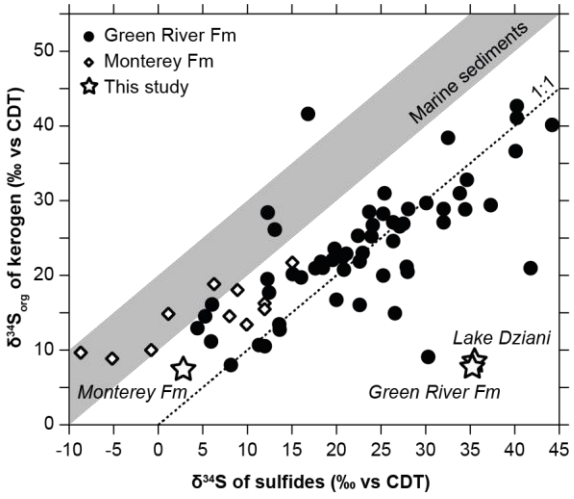
Green River Fm
Monterey Fm
This study
Marine sediments
1:1
Lake Dziani
Monterey Fm
Green River Fm
δ34Sorg of kerogen (‰ vs CDT)
δ34S of sulfides (‰ vs CDT)
0
10
20
30
40
50
-10
-5
0
5
10
15
20
25
30
35
40
45

Figure 7

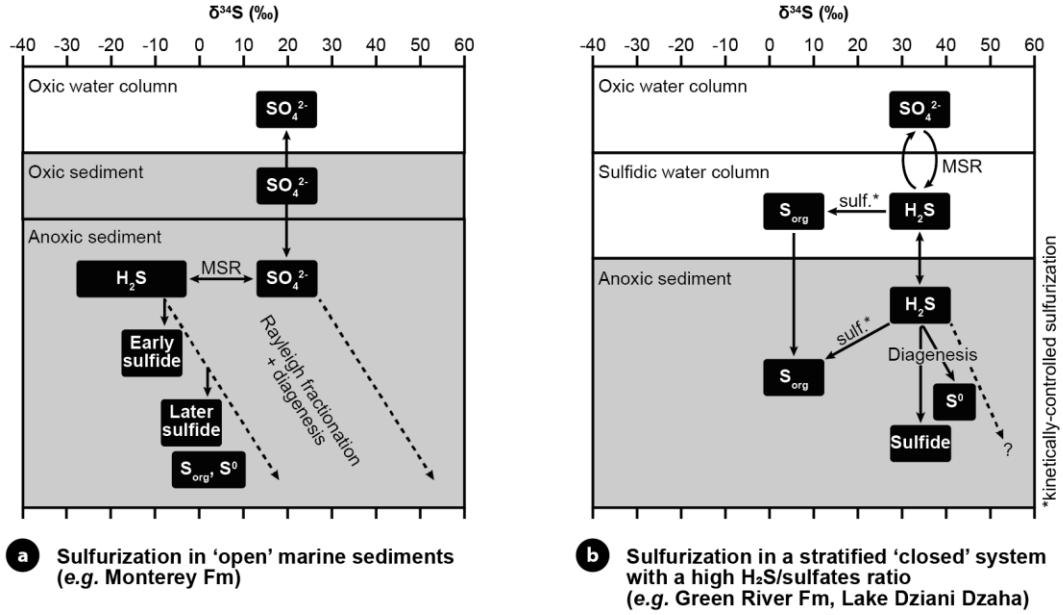
δ³⁴S (‰)
-40 -30 -20 -10 0 10 20 30 40 50 60
Oxic water column
SO4 2-
Oxic sediment
SO4 2-
Anoxic sediment
H2S
MSR
SO4 2-
Early sulfide
Later sulfide
Sorg, S0
Rayleigh fractionation + diagenesis
a
Sulfurization in 'open' marine sediments (e.g. Monterey Fm)
δ³⁴S (‰)
-40 -30 -20 -10 0 10 20 30 40 50 60
Oxic water column
SO4 2-
MSR
Sulfidic water column
Sorg
sulf.*
H2S
Anoxic sediment
H2S
sulf.*
Diagenesis
Sorg
S0
Sulfide
?
*kinetically-controlled sulfurization
b
Sulfurization in a stratified 'closed' system with a high H2S/sulfates ratio (e.g. Green River Fm, Lake Dziani Dzaha)

Figure 8